Bull. Mater. Sci., Vol. 36, No. 6, November 2013, pp. 967–972.

Detection of H_2S gas at lower operating temperature using sprayed nanostructured In_2O_3 thin films

RAMESH H BARI*, **PARAG P PATIL**, **SHARAD B PATIL** and **ANIL R BARI**[†]

Department of Physics, G. D. M. Arts, K. R. N. Commerce and M. D. Science College, Jamner 424 206, India

[†]Department of Physics, Arts, Commerce and Science College, Bodwad 425 310, India

MS received 23 March 2012; revised 8 May 2012

Abstract. **Nanostructured indium oxide (In_2O_3) thin films were prepared by spray pyrolysis (SP) technique. X-ray diffraction (XRD) was used to investigate the structural properties and field emission scanning electron microscopy (FESEM) was used to confirm surface morphology of In_2O_3 films. Measurement of electrical conductivity and gas sensing performance were conducted using static gas sensing system. Gas sensing performance was studied at different operating temperature in the range of 25–150 °C for the gas concentration of 500 ppm. The maximum sensitivity ($S = 79\%$) to H_2S was found at lower temperature of 50 °C. The quick response (4 s) and fast recovery (8 s) are the main features of this film.**

Keywords. **Nanostructured In_2O_3; thin films; spray pyrolysis; H_2S gas sensor; low temperature.**

1. Introduction

Hydrogen sulphide (H_2S) is a toxic and inflammable gas, produced in sewage plants, coal mines and oil and natural gas industries. It is used in large amounts in various chemical industries, research laboratories and as a process gas in the production of heavy water (Kaur *et al* 2008). Presently, the atmospheric pollution has become a global burning issue. Gases from automobiles and industrial exhausts are polluting the environment. In particular, indium oxide is promising material for detection of various substances, e.g. LPG, H_2, CO_2, NH_3, C_2H_5OH, CH_3OH, Cl_2 and H_2S. Furthermore, nanostructured materials present new opportunities for enhancing the properties and performance of gas sensors and are recognized as essential for achieving high gas sensitivity.

Indium oxide thin film is a technologically important transparent conducting oxide (TCO) material (Riveros *et al* 2006). In_2O_3 is used in different fields like: photovoltaic devices, transparent windows in liquid crystal displays, sensors, anti-reflection coatings (Chopra *et al* 1983) and electrochromic devices (Sharma *et al* 2009). Thin films of In_2O_3 can be prepared by a variety of techniques such as chemical vapour deposition (Kane and Schweitzer 1975) spray pyrolysis (Manifacier *et al* 1979) vacuum evaporation (Murali *et al* 2002) and magnetron sputtering (Haines and Bube 1978).

Among these techniques, spray pyrolysis technique compete with others due to its low cost, suitable properties and process well suited to large scale production. It has several advantages in producing nanocrystalline thin films suitable for the gas sensors, such as, relatively homogeneous composition, easy control of film thickness and fine and porous microstructure. In this work, nanocrystalline In_2O_3 thin films with different spraying time of the solution were prepared by spray pyrolysis technique. Crystal structure and grain sizes were studied from X-ray diffraction and FESEM. These nanocrystalline In_2O_3 thin films were tested for sensing different conventional gases and were observed to be most sensitive to H_2S at 50 °C.

2. Experimental

2.1 *Preparation of nanocrystalline In_2O_3 thin films*

Indium oxide thin films were prepared using spray pyrolysis technique. The films of various thicknesses were deposited by varying deposition time of solution between 10 and 40 min. The solution was prepared by dissolving indium trichloride ($InCl_3$) [Alfa Aesar] in deionized water and adding 1–3 drops of concentrated HCl to clean the precipite so as to get desired solution concentration (0·025 M). The spray produced by nozzle was sprayed onto the glass substrates heated at 250 ± 5 °C. Various parameters such as solution concentration (0·025 M), spray rate (5 mL/min), nozzle to and fro frequency (16 cycles/min), nozzle to substrate distance (30 cm), etc were optimized to obtain good quality films. This resulted in the formation of well adherent, transparent and uniform indium oxide thin films. The films with different deposition time of: 10, 20, 30 and 40 min were obtained and referred to as S1, S2, S3 and S4, respectively in text. The samples were fired at 500 °C for 1 h.

*Author for correspondence (rameshbari24@yahoo.com)

2.2 *Chemical reaction*

The indium oxide formulation can be represented as:

$$2InCl_3 + 3H_2O \longrightarrow In_2O_3 + 6HCl \ (gas)\uparrow. \quad (1)$$

2.3 *Sensing system for measurement of gas sensitivity*

The gas sensing studies were carried out using a static gas chamber to sense H_2S gas in air ambient. The nanostructured SnO_2 thin films were used as the sensing elements. Cr–Al thermocouple is mounted to measure the temperature. The output of thermocouple is connected to temperature indicator. Gas inlet valve fitted at one of the ports of base plate. Gas concentration inside the static system is achieved by injecting a known volume of test gas in gas injecting syringe. Constant voltage is applied to the sensor and current can be measured by picoammeter.

2.4 *Characterization of thin films*

The nanostructured In_2O_3 thin films were characterized by X-ray diffraction (Miniflex Model, Rigaku, Japan) using CuKα radiation with a wavelength, $\lambda = 1{\cdot}5418$ Å. The microstructure of the films was analysed using a field emission scanning electron microscope (FE–SEM, JEOL, JED 6300). Thermoelectric power measurement was carried out using TEP set up. Electrical and gas-sensing properties were measured using a static gas sensing system. The sensor performance on exposure of LPG, carbon dioxide, hydrogen, ammonia, ethanol, chlorine and H_2S was examined.

Table 1. Variation of activation energy and thickness with spray time (thickness).

Sample	Spray time	Thickness (nm)	Activation energy (eV) (temperature range 40–150 °C)
1	10	153	0·561
2	20	169	0·515
3	30	172	0·461
4	40	189	0·369

3. Results and discussion

3.1 *Measurement of films thickness*

Film thickness was measured by using a micro-gravimetrical method (Sartale and Lokhande 2001). The films were deposited on clean glass slides whose mass was previously determined. After the deposition, the substrate was again weighed, determining the quantity of deposited indium oxide. Measuring the surface area of the deposited film, taking account of indium oxide specific weight of the film, thickness was determined using the relation:

$$T = M_{In_2O_3}/A * \rho * 10^4, \quad (2)$$

where A is the surface area of the film (cm^2), $M_{In_2O_3}$ the quantity of the deposited tin oxide and ρ the specific weight of indium oxide. Measurements of film thickness with deposition spray time are given in table 1.

3.2 *Thermoelectric power measurements*

The p- or n-type semiconductivity of the thin films of In_2O_3 were confirmed by measuring the thermoelectric power of the thin film samples. The In_2O_3 were observed to be the n-type material.

3.3 *Structural properties*

The structural characterization of deposited films was made by X-ray diffraction (XRD) technique with monochromatic CuKα radiation, $\lambda = 1{\cdot}5418$ Å. The XRD patterns were

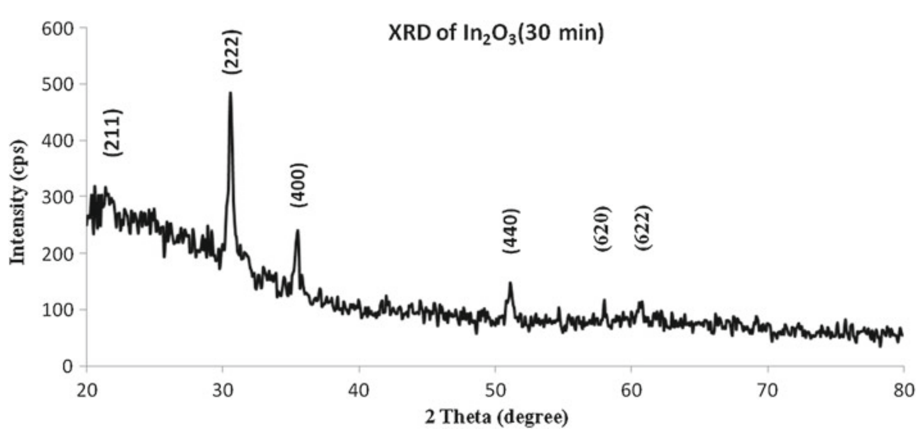

Figure 1. X-ray diffractogram of most sensitive indium oxide thin film.

recorded in 2θ interval from 20 up to 80° with a step of 0·05°. Figure 1 shows X-ray diffractogram of nanocrystalline indium oxide thin film. The observed peaks: (211), (222), (400), (440), (620) and (622) are very well matching with JCPDS data of indium oxide (JCPDS data card no. 44-1087) possessing cubic structure. It is seen from the figure that the films exhibited strong orientation along (222). The average crystalline size calculated from Scherrer's formula was found to be 23 nm.

3.4 *Microstructure study*

The surface topography of the films was analysed using a field emission scanning electron microscopy as shown in figure 2(a and b).

The morphology of the particles was roughly spherical in shape. The average particle size was about 36 nm. Larger particles may be due to the agglomeration of smaller crystallites as shown in the low magnification image as in figure 2(a and b) shows the high magnification image, indicating the sphere associated with smaller crystallites.

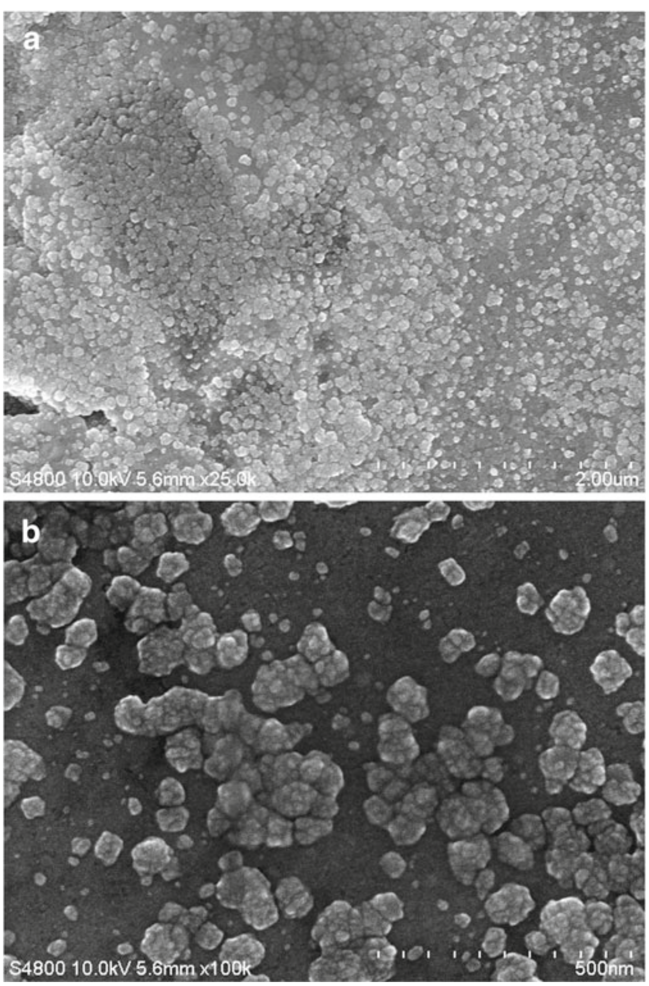

Figure 2. FESM images of nanostructured indium oxide thin film sample: (**a**) low magnification and (**b**) high magnification.

3.5 *Electrical properties*

3.5a *I–V characteristics*: Figure 3 shows I–V characteristics of samples $S1$, $S2$, $S3$ and $S4$ observed to be nearly symmetrical in nature indicating ohmic nature of contacts. The non-linear I–V characteristics may be due to semiconducting nature of the thin film samples.

3.5b *Electrical conductivity*: Figure 4 shows variation of log (conductivity) with an operating temperature. The conductivity of each sample is observed to be increasing with an increase in temperature. The increase in conductivity with increase in temperature could be attributed to negative temperature coefficient of resistance and semiconducting nature of nanocrystalline In_2O_3. It is reported (Sharma and Garg 1990; Mandouh and Mandouh 1995) that there is variation of activation energy with thickness. As the thickness of the film increases the activation energy goes on decreasing. The activation energy calculated from slopes of line for 10, 20, 30 and 40 min thin films were found to be 0·561, 0·515, 0·461 and 0·369 eV, respectively.

3.6 *Gas sensing performance*

3.6a *Sensitivity*: It is defined as the change in conductance of the sample on exposure to gas to the original conductance. It is given by the relation:

$$S\,(\%) = \frac{G_a - G_g}{G_a} = \frac{\Delta G}{G_a}, \tag{3}$$

where G_a is the conductance of sensor in air and G_g the conductance of sensor in presence of gas.

Figure 5 shows variation of sensitivity with operating temperature of samples $S1$, $S2$, $S3$ and $S4$ on exposure to

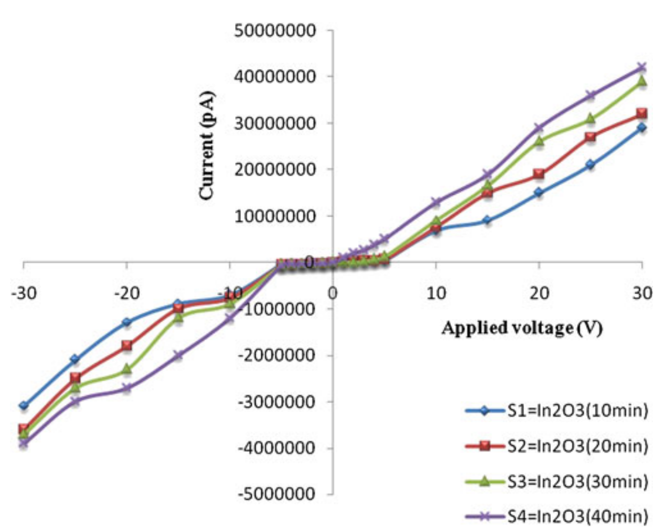

Figure 3. I–V characteristics of nanocrystalline indium oxide thin film sensors.

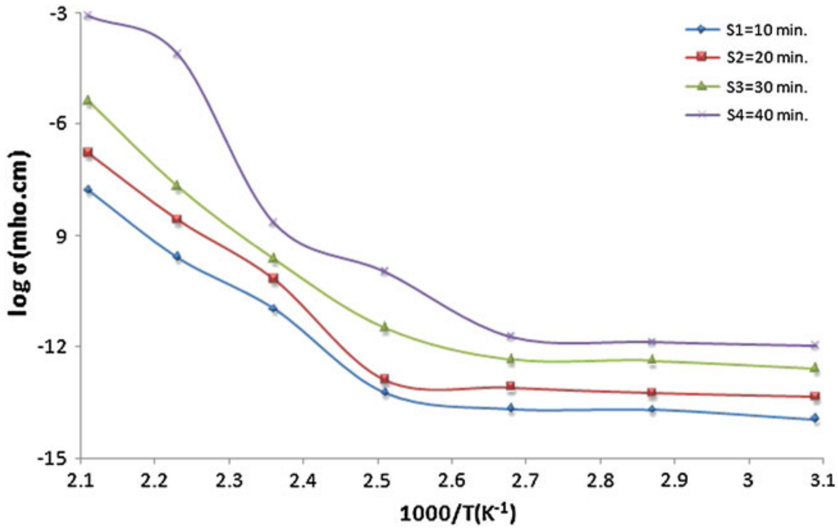

Figure 4. Variation of log (conductivity) with operating temperature (°C).

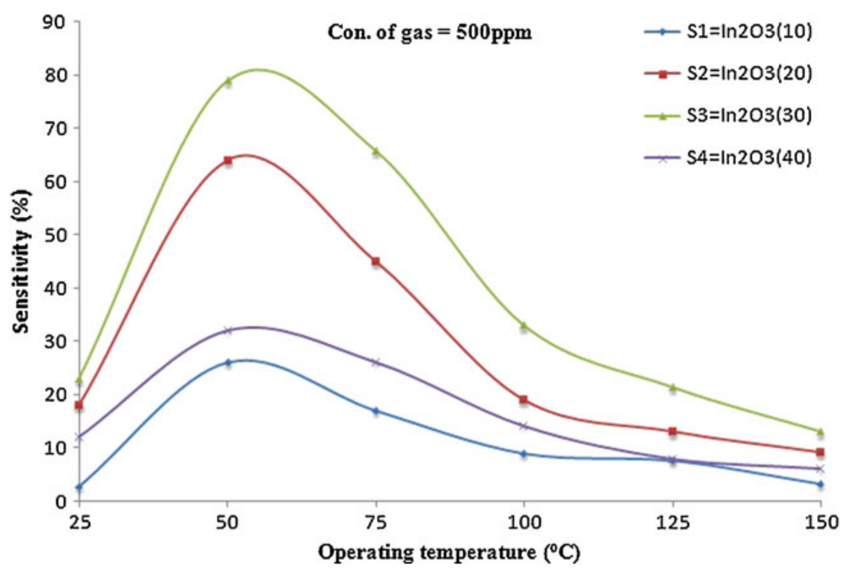

Figure 5. Sensitivity of pure nanostructured indium oxide thin films with operating temperature.

500 ppm H_2S. It is clear from figure 5 that the H_2S sensitivity of sample $S3$ is higher ($S = 79\%$) at 50 °C as compared to those of $S1$, $S2$ and $S4$. It is well known that the sensitivity of the metal–oxide semiconductor sensors is mainly determined by the interactions between a target gas and the surface of the sensors. Due to the greater surface area of nanostructured materials, its interaction with the adsorbed gases is stronger, leading to higher gas response.

3.6b *Selectivity*: The response of the sensor to a specific gas in the mixture of gases is the selectivity.

Selectivity of nanocrystalline indium oxide thin film sensors is measured at an operating temperature of 50 °C. Figure 6 depicts bar diagram to indicate H_2S selective ability of the sensor. It is clear from the figure that the responses of all samples to LPG, CO_2, H_2, NH_3, C_2H_5OH, CH_3OH and Cl_2 gases are lower as compared to their response to H_2S. Nanocrystalline indium oxide thin films are, therefore, highly selective to H_2S.

3.6c *Response and recovery of sensor*: The time taken by the sensor to attain the 80% of maximum change in resistance on exposure to the gas is response time. The time taken by the sensor to roll back to 80% of its original resistance is the recovery time.

The response and recovery of the nanostructured indium oxide thin film ($S3$) sensor on exposure of 500 ppm of H_2S at 50 °C are represented in figure 7. The response is quick (4 s) and recovery is fast (8 s).

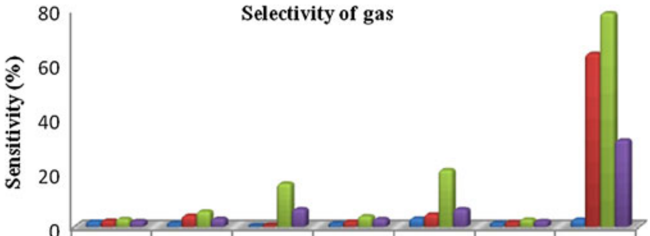

	LPG	CO_2	H_2	NH_3	C_2H_5OH	Cl_2	H_2S
S1	1.9	1.3	0.26	1.2	3.1	1.4	2.7
S2	2.3	4.13	0.5	1.9	4.6	1.6	64
S3	2.9	5.69	16	3.9	21	2.74	79
S4	2.1	3	6.5	2.9	6.5	2.1	32

Figure 6. Selectivity of nanostructured indium oxide thin films for different gases.

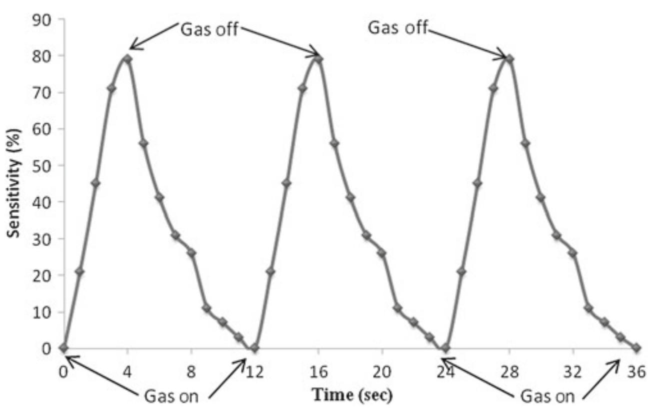

Figure 7. Response and recovery of sensor.

3.7 *Discussion*

The gas-sensing mechanism of In_2O_3-based thin films belongs to the surface controlled type, which is based on the change in conductance of the semiconductor. The oxygen adsorbed on the surface directly influences the conductance of the In_2O_3-based sensors as shown in figure 8.

The amount of oxygen adsorbed on thin film surface depends on the operating temperature, particle size and specific surface area of sensor. The state of oxygen on the surface of In_2O_3 thin film undergoes the following reaction:

$$O_2\ (gas) \longrightarrow O_2\ (ads), \tag{4}$$

$$O_2\ (ads) + e^- \longrightarrow O_2^-\ (ads), \tag{5}$$

$$O^- + e^- \longrightarrow O^{2-}\ (ads). \tag{6}$$

The oxygen species capture electrons from the material, which results in the concentration changes of holes or electrons in the In_2O_3 semiconductor. When the In_2O_3 thin film is exposed to H_2S gas, the reductive gas reacts with the oxygen adsorbed on the thick film surface. Then, the electrons are released back into the semiconductor, resulting in the change in the electrical conductance of In_2O_3 thin films. It can be expressed in the following reaction:

$$H_2S + 3O \longrightarrow H_2O + SO_2 + 6e. \tag{7}$$

In_2O_3 thin film when exposed to H_2S gas, conductivity would be very low in air and very high on exposure to H_2S gas and therefore, the gas response would be highest for In_2O_3 thin film. For the In_2O_3 thin film, the low gas response at low operating temperature can be attributed to the low thermal energy of the gas molecules, which is not enough to react with the surface adsorbed oxygen species. As a result, the reaction rate between them is essentially low and low gas response is observed. On the other hand, the reduction in response after the optimum operating temperature may be due to the difficulty in exothermic gas adsorption at higher temperature and as a result, the initial resistance of thin film would decrease and the overall change in resistance on exposure to gas would be smaller leading to lower response to the target gas (Patil *et al* 2010, 2012). Uniform and optimum dispersion of an additive dominates the depletion of electrons from semiconductor. Oxygen adsorbing on additive (misfits) removes electrons from the additive and additive in turn removes the electron from the nearby surface region of the semiconductor and could control the conductivity.

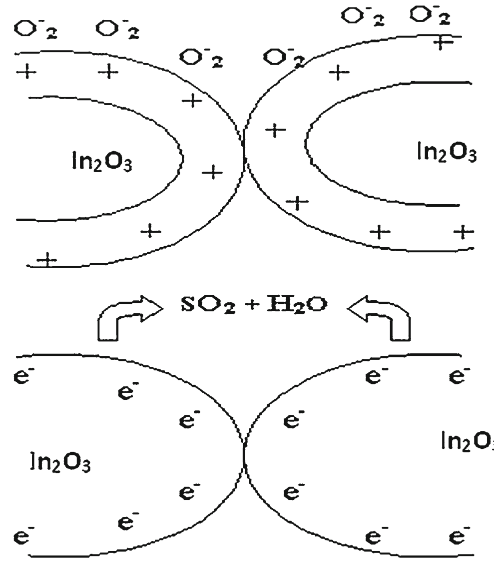

Figure 8. H_2S gas sensing mechanism.

4. Conclusions

(I) Nanostructured indium oxide thin films could be prepared by simple and inexpensive spray pyrolysis technique.

(II) The structural and microstructural properties confirm that the as-prepared indium oxide thin films are nanostructured in nature.
(III) The indium oxide thin film of (sample $S3 = 30$ min spray time) was most sensitive to H_2S gas and exhibit the response of $S = 79\%$ to the gas concentration of 500 ppm at the temperature of 50 °C.
(IV) The sensor has good selectivity to H_2S against LPG, CO_2, H_2, NH_3, ethanol, methanol and Cl_2.
(V) The nanostructured indium oxide thin films exhibit rapid response–recovery.
(VI) Low operating temperature, highly selective and rapid response–recovery are the main features of this sensor.

Acknowledgements

The authors are thankful to the University Grants Commission, New Delhi for providing financial support. Thanks to Principal, G D M Arts, K R N Commerce and M D Science College, Jamner, for providing laboratory facilities to this work.

References

Chopra K L, Major S and Pandya D K 1983 *Thin Solid Films* **102** 1
Haines W G and Bube R H 1978 *J. Appl. Phys.* **49** 304
Kane J and Schweitzer H P 1975 *Thin Solid Films* **29** 55
Kaur M, Jain N, Sharma K, Bhattacharya S, Royb M, Tyagib A K, Gupta S K and Yakhmia J V 2008 *Sens. Actuators B: Chem.* **133** 456
Manifacier J C, Szepessy L, Bresse J F, Peroten M and Stuck R 1979 *Mater. Res. Bull.* **14** 109
Mandouh Z S and Mandouh M 1995 *FIZIKAA* **4** 17
Murali K R, Sambasivam V, Jayachandran M, Chockalingam M J, Rangarajan N and Venkatesan V K 2002 *J. Cryst. Growth* **240** 142
Patil L A, Bari A R, Shinde M D, Deo Vinita and Kaushik M P 2012 *Sens. Actuators B: Chem.* **161** 372
Patil L A, Bari A R, Shinde M D and Deo Vinita 2010 *Sens. Actuators B: Chem.* **149** 79
Riveros R, Romero E and Gordillo G 2006 *Brazilian J. Phys.* **36** 102
Sartale S D and Lokhande C D 2001 *Mater. Chem. Phys.* **72** 101
Sharma K C and Garg J C 1990 *Phys. D: Appl. Phys.* **23** 1411
Sharma R, Mane R S, Min S K and Han S H 2009 *J. Alloys Compd.* **479** 840